A&A 457, 335–341 (2006)
DOI: 10.1051/0004-6361:20065445

Astronomy & Astrophysics

Confirmation of the planet hypothesis for the long-period radial velocity variations of β Geminorum[⋆,⋆⋆]

A. P. Hatzes[1], W. D. Cochran[2], M. Endl[2], E. W. Guenther[1], S. H. Saar[3], G. A. H. Walker[4], S. Yang[5], M. Hartmann[1], M. Esposito[1], D. B. Paulson[6], and M. P. Döllinger[7]

[1] Thüringer Landessternwarte Tautenburg, Sternwarte 5, 07778 Tautenburg, Germany
e-mail: artie@tls-tautenburg.de
[2] McDonald Observatory, The University of Texas at Austin, Austin, TX 78712, USA
[3] Harvard-Smithsonian Center for Astrophysics, 60 Garden Street, Cambridge, MA 02138
[4] 1234 Hewlett Place, Victoria, BC, V8S 4P7, Canada
[5] Department of Physics and Astronomy, University of Victoria, Victoria, BC, V8W 3P6, Canada
[6] Planetary Systems Branch, Code 693, NASA Goddard Space Flight Center, Greenbelt, MD 20771, USA
[7] European Southern Observatory, Karl-Schwarzschild-Straße 2, 85748 Garching bei München, Germany

Received 18 April 2006 / Accepted 16 June 2006

ABSTRACT

Aims. Our aim is to confirm the nature of the long period radial velocity measurements for β Gem first found by Hatzes & Cochran (1993).
Methods. We present precise stellar radial velocity measurements for the K giant star β Gem spanning over 25 years. An examination of the Ca II K emission, spectral line shapes from high resolution data (R = 210 000), and Hipparcos photometry was also made to discern the true nature of the long period radial velocity variations.
Results. The radial velocity data show that the long period, low amplitude radial velocity variations found by Hatzes & Cochran (1993) are long-lived and coherent. Furthermore, the Ca II K emission, spectral line bisectors, and Hipparcos photometry show no significant variations of these quantities with the radial velocity period. An orbital solution assuming a stellar mass of 1.7 $M_{\odot}$ yields a period, P = 589.6 days, a minimum mass of 2.3 $M_{\rm Jupiter}$, and a semi-major axis, a = 1.6 AU. The orbit is nearly circular (e = 0.02).
Conclusions. The data presented here confirm the planetary companion hypothesis suggested by Hatzes & Cochran (1993). β Gem is one of six intermediate mass stars known to host a sub-stellar companion and suggests that planet-formation around stars much more massive than the sun may common.

Key words. star: individual: β Gem – techniques: radial velocities – planetary systems

1. Introduction

Long-period, low amplitude radial velocity (RV) variations were reported in three K giant stars, including β Gem (= Pollux = HR 2990 = HD 62509) by Hatzes & Cochran (1993) (hereafter HC93). One hypothesis for the RV variations was the presence of planetary companions. In the case of β Gem an orbital solution yielded a minimum mass $m \sin i$ = 2.9 $M_{\rm Jupiter}$ (assuming a stellar mass of M = 2.8 $M_{\odot}$), semi-major axis, a = 1.9 AU and eccentricity, e = 0.12. Hatzes & Cochran noted that "...it would seem that planetary companions around K giants have been detected". However, since RV variations of comparable periods were also found for α Boo and α Tau, HC93 were cautious in the interpretation: "...it seems improbable that all three would have companions with similar masses and periods unless planet formation around the progenitors to K giants was an ubiquitous phenomenon". Indeed, up until that time extrasolar planet RV searches were yielding no detections, even around main-sequence stars, so it seemed odd that K giant stars would produce an abundance of sub-stellar companions. This, and the fact that the expected rotation periods of K giant stars were comparable to the detected long period RV variations made rotational modulation by stellar surface structure a viable alternative.

Subsequent work by Larson et al. (1993b) confirmed the long period RV variations of β Gem with a revised period of 585 days. That work also showed that the Ca II λ8662 equivalent width varied at the few percent level with the same period as the RV variations. This seemed to support rotational modulation by surface structure as a cause of the RV variations, although the Ca II equivalent width variations were marginal. The false alarm probability for the signal was about 1% and Larson et al. commented: "However, because of the weakness of the signal, $K = 0.583 \pm 0.19$ mÅ, this signal needs confirmation".

Since the discovery of RV variations in β Gem, planetary companions have been established in several K giant stars. The planetary companion to ι Dra (Frink et al. 2002) was largely accepted because of the eccentric orbit, a shape in the RV curve that is difficult to produce with rotational modulation. Companions to HD 47536 (Setiawan et al. 2003), HD 11977 (Setiawan et al. 2005), and HD 13189 (Hatzes et al. 2005) were established by the absence of Ca II H & K emission and the lack of spectral line bisector variations with the same period as the RV.

⋆ Based in part on observations obtained at the 2-m-Alfred Jensch Telescope at the Thüringer Landessternwarte Tautenburg and the Harlan J. Smith 2.7 m telescope of McDonald Observatory.
⋆⋆ Tables 2–4 are only available in electronic form at http://www.edpsciences.org

Over a decade since their discovery the nature of the long period variations in β Gem is still unknown. For these reasons we continued to monitor this star with precise stellar radial velocity measurements. These new measurements along with previous ones span over 25 years in time. In Sect. 3 we show that the RV variations in this star first reported in 1993 are still present with the same period and amplitude. In Sect. 4 we make a careful analysis of ancillary data that were available to us. These are Ca II K emission, Hipparcos photometry, and spectral line bisectors measured using very high spectral resolution data. Our analysis demonstrates that there are no other forms of variability with the same period as the RV variations. This confirms the planet hypothesis for this star first reported by HC93.

2. The star

β Gem is a K0 III star at a distance of 10.3 pcs as measured by Hipparcos. Interferometric measurements have determined an angular diameter of 7.96 ± 0.09 mas (Nordgren et al. (2001) which corresponds to a radius of $8.8 \pm 0.1\ R_{\odot}$ The atmospheric parameters for this star have been derived by several investigators. McWilliam (1990) measured an effective temperature of 4850 K, a metallicity of [Fe/H] = −0.07, and a surface gravity, $\log g = 2.96$. Gray et al. (2003) derived the same effective temperature, but a lower surface gravity ($\log g = 2.52$) and higher metallicity ([Fe/H] = 0.08). More recently, Allende-Prieto et al. (2004) determined $T_{\rm eff} = 4666 \pm 95$ K, a surface gravity of $\log g = 2.685 \pm 0.09$ and a metallicity, [Fe/H] = 0.19, a value considerably higher than previous determinations.

Allende Prieto & Lambert (1999) derived a stellar mass of $M = 1.7 \pm 0.4\ M_{\odot}$, a value we shall adopt. We are aware that the determination of the stellar mass for giant stars is difficult. This relies not only on an accurate measurement of stellar parameters, but also on the reliability of evolutionary models. Since main sequence stars with spectral types in the range A–G can all evolve to K giant status, the true mass of β Gem may be outside the range of the nominal error given by Allende Prieto & Lambert. They also derived a stellar radius of $R = 8.9 \pm 0.4\ R_{\odot}$, a value consistent with interferometric measurements.

3. The radial velocity data

Six independent data sets of high precision radial velocity data were used for our analysis. Three data sets have already been published. Larson et al. (1993b) used data from the Canada France Hawaii Telescope (CFHT) survey as well as data taken at the Dominion Astrophysical Observatory (DAO). The DAO data had a RV precision about a factor of 2 worse than the CFHT measurements as well as the ones we present here. These data span the time 1980–1993. The McDonald Observatory measurements that appeared in the discovery paper of HC93 were made at the 2.1 m telescope (McD-2.1 m). These data span the time period 1980–1992. New measurements were obtained at McDonald Observatory and the Thuringia State Observatory (Thüringer Landessternwarte). Table 1 lists the journal of observations which includes the data set, time coverage, the RV technique employed, and the number of observations. The CFHT and DAO measurements employed a hydrogen fluoride (HF) absorption cell (Campbell & Walker 1979). All other data sets utilized the iodine absorption cell (I2) for the wavelength reference. Table 1 also lists the rms scatter of the points about the orbital solution (see below). These standard deviations represent the true measurement error as well as any intrinsic variability of star on time scales much shorter than the long period found in the data.

Table 1. The data sets used in the orbital solution.

Data Set	Coverage	Technique	N	σ_{RV} (m s^{-1})
CFHT	1980.87–1991.87	HF cell	24	20.3
DAO	1985.28–1993.05	HF cell	25	37.7
McD-2.1 m	1988.73–1992.20	Iodine Cell	31	18.9
McD-MOPS	1998.69–2000.03	Iodine Cell	22	11.6
McD-cs21	2000.03–2004.58	Iodine Cell	11	16.7
TLS-TOPS	2003.04–2006.06	Iodine Cell	22	11.0

Two of the new data sets were obtained from McDonald Observatory. The first set was taken as part of the Phase III radial velocity program of the McDonald Observatory Planet Search (MOPS) program that used the "low resolution" mode of the 2dcoudé cross-dispersed echelle spectrograph (Tull et al. 1994) at the Harlan J. Smith 2.7m telescope. This instrument, when used with a Tektronix 2048×2048 detector, provides a nominal wavelength coverage of 3600 Å – 1 μm at a resolving power of R ($=\lambda/\Delta\lambda$) = 60 000. The RV-information from the I_2 self-calibrated spectra taken during Phase III was obtained using the *Austral* RV-code (Endl et al. 2000). The data from the McDonald Phase III are given in Table 2. The uncertainties quoted there and in other tables are the "internal" errors as represented by the the rms scatter of the individual spectral chunks (∼several hundred) used in the RV calculation (see Endl et al. 2000). We regard these as a lower limit on the actual uncertainties, since these values do not include the effects of any residual systematic errors or stellar "jitter" that may be present.

The second set of McDonald data were taken using the high resolution mode of the 2dcoudé cross-dispersed echelle spectrograph (often referred to as the cs21 focus and referred to as "cs21" in the tables and figures). This setup provided a resolving power, $R = 210\,000$ using the same Tektronix CCD detector, although with much more limited wavelength coverage (about 800 Å). These data were primarily taken for an examination of the spectral line shapes, although some observations were made with the iodine cell so as to correlate any RV variations with changes in the spectral line shapes. Table 3 lists the RVs made with the high resolution mode of the 2dcoudé.

Finally, observations of β Gem were made as part of the Tautenburg Observatory Planet Search (TOPS) program. This uses the high resolution coudé echelle spectrometer of the Alfred-Jensch 2m telescope and an iodine absorption cell placed in the optical path. This is a grism crossed-dispersed echelle spectrometer that has a resolving power R ($\lambda/\Delta\lambda$) = 67 000 and wavelength coverage 4630–7370 Å when using the so-called "Visual" grism. A more detailed description of radial velocity measurements from the TOPS program can be found in Hatzes et al. (2005). Table 4 lists RV measurements of β Gem from the TOPS program.

The RV measurements for all data sets are shown in Fig. 1. Each data set had its own velocity offset that had to be applied so that they would all have the same zero point (see below, the tabulated values have the offsets applied). There is a clear sinusoidal variation that persists over the entire time span covered by the data.

Figure 2 shows the Lomb-Scargle periodogram (Lomb 1976; Scargle 1982) of all the RV measurements. These show a dominant peak at a frequency of $\nu = 0.0017$ c d^{-1} (period = 590 d). The false alarm probability (FAP) of this peak using the expressions in Scargle (1982) is FAP $\approx 10^{-16}$. With such large Lomb-Scargle power it is pointless to perform Monte Carlo

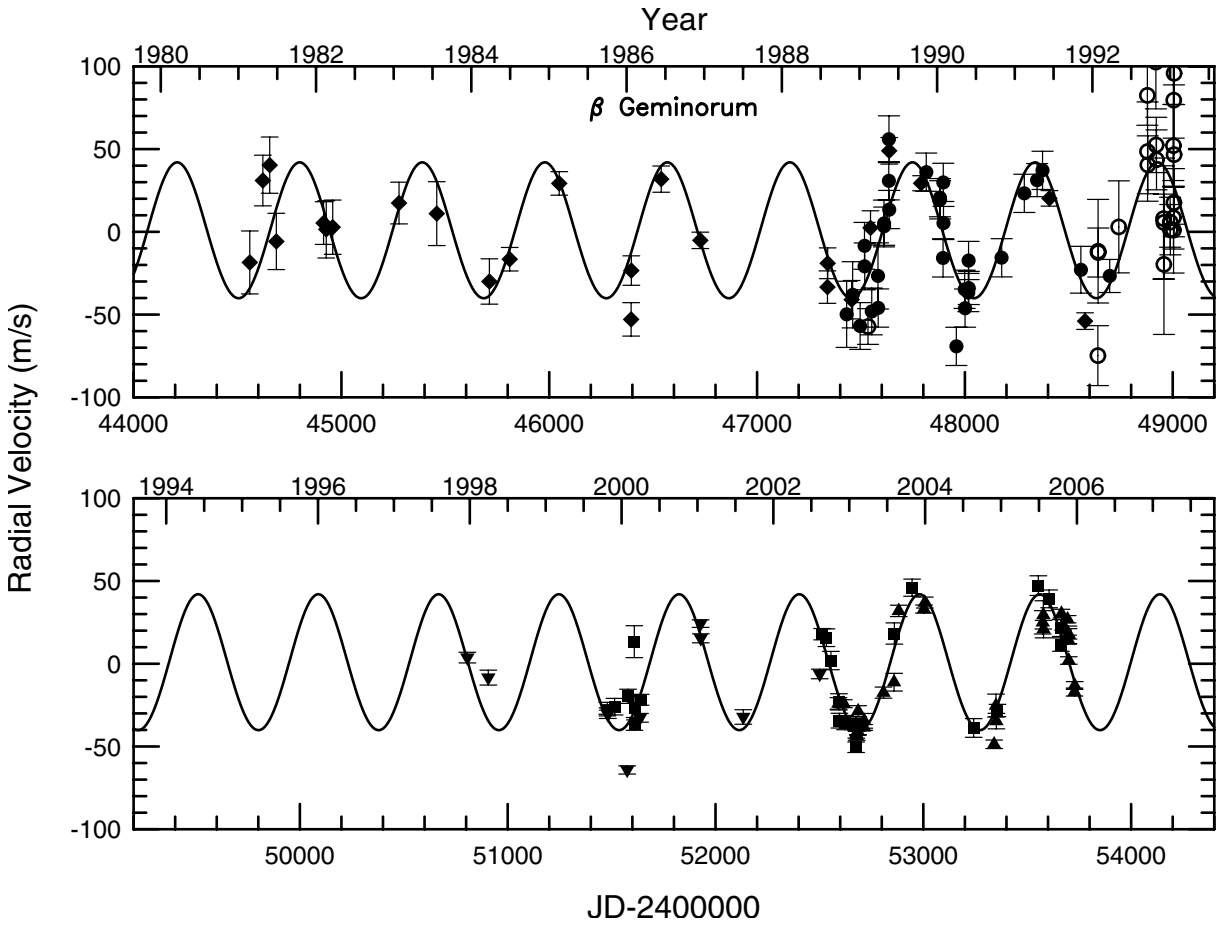

Fig. 1. Radial velocity measurements for β Gem from the 6 data sets: CFHT (diamonds), DAO (dots), McD-2.1 m (circles), McD-cs21 (inverted triangles), McD-MOPS (squares), and TOPS (triangles).

simulations of the FAP. Nevertheless, the FAP was also was determined using the bootstrap randomization technique (Murdoch et al. 1993; Kürster et al. 1997). The measured RV values were randomly shuffled keeping the observed times fixed and a periodogram for the shuffled data computed. The fraction of the random periodograms having power higher than the data periodogram yields the false alarm probability that noise would create the detected signal. As expected, after 2×10^5 "shuffles" there was no instance where the random periodogram had more Lomb-Scargle power than the data. This FAP is indeed very small.

4. Orbital solution

An orbital solution was calculated using the combined data sets. This is shown by the solid line in Fig. 1. The velocity zero point for each data set was allowed to be a free parameter. This was varied until the best fit in a least-squares sense was obtained. These individual zero points in the velocity were subtracted from each data set before plotting in Fig. 1. The orbital parameters are listed in Table 5. The rms scatter listed for the orbital solution is from the combined data sets. Figure 3 shows the RV measurements of each data set phased to the orbital period. We should note that a significant fraction of the the rms scatter may be due to intrinsic variability. K giants are known to exhibit stellar oscillations with periods of 0.25–10 days and amplitudes of 10–100 m s^{-1} (Hatzes & Cochran 1994a,b, 1995; Kim et al. 2006).

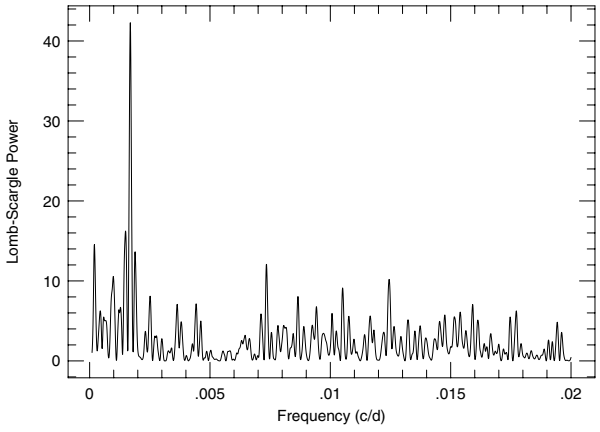

Fig. 2. Lomb-Scargle periodogram of the combined RV data sets.

5. The nature of the RV variations

The fact that the RV variations seem to be long-lived and coherent for over 25 years strongly argues that they are indeed due to a sub-stellar companion. However, β Gem is a giant star and we know little about the nature of possible surface structure on these type of stars or how long-lived they might be. An exotic form of long-period stellar oscillation can also not be excluded. Furthermore, the weak Ca II λ8662 variations found by Larson et al. (1993b) compels us to be cautious about the interpretation of the RV variations. To confirm that a sub-stellar

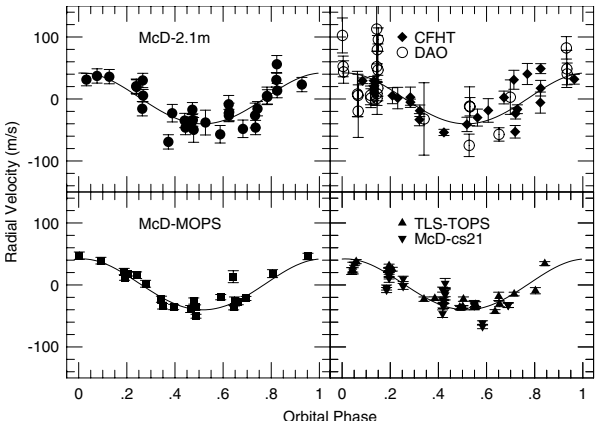

Fig. 3. Radial velocity measurements for β Gem from the 6 data sets phased to the orbital period. The symbols are the same as for Fig. 1.

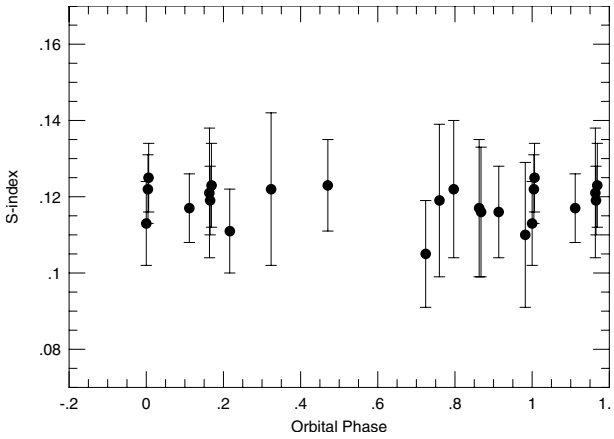

Fig. 4. McDonald S-index measurements for β Gem phased to the 590-day orbital period. Points are repeated for the second cycle.

Table 5. Orbital parameters for the companion to β Gem. The rms scatter in parenthesis is without the DAO measurements.

Parameter	Value
Period [days]	589.64 ± 0.81
$T_{\rm periastron}$ [JD]	2 447 739.02 ± 4.5
K [m s^{-1}]	41.0 ± 1.6
e	0.02 ± 0.03
ω [deg]	354.58 ± 95.65
$f(m)$ [solar masses]	$(4.21 \pm 0.48) \times 10^{-9}$
$m \sin i$ [$M_{\rm Jupiter}$]	2.30 ± 0.45
a [AU]	1.64 ± 0.27
rms [m s^{-1}]	20.6 (17.1)

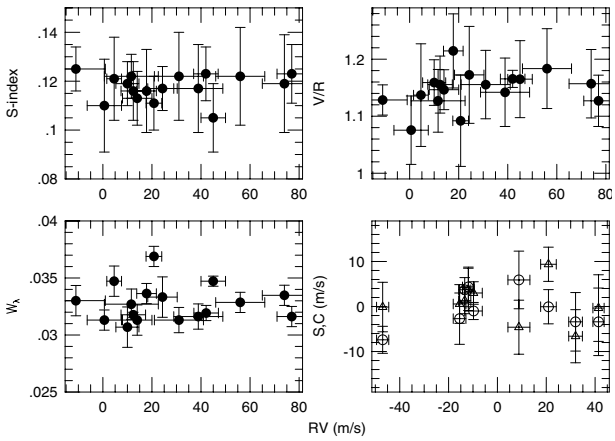

Fig. 5. Correlation of the radial velocity with S-index (*top left panel*), ratio of emission peaks in Ca II, V/R (*top right panel*), equivalent width of core Ca II emission (*bottom left panel*), and velocity span, S (circles) and curvature, C (triangles) of the spectral line bisector (*lower right panel*).

companion is indeed responsible for the RV variations we examined the Ca II K emission, the spectral line shapes, and the Hipparcos photometry to see if any of these correlated with the RV variations.

5.1. Ca II emission

Larson et al. (1993b) found variations in the equivalent width of Ca II 8662 that showed a long term trend on a timescale greater than 12 years. This was fit with a quadratic polynomial plus sinusoid that had the same period as the RV variations. As stated earlier their periodogram of the Ca II equivalent width measurements after subtracting the long term showed only marginal power at the RV period. Larson et al. (1993a) showed that their Ca II 8662 measurements gave results consistent with the Mt. Wilson S-index measurements. The wavelength coverage of the McDonald Phase III data included the Ca II K line, a feature traditionally used for measurement of stellar chromospheric variability. Paulson et al. (2002) defined an S-index that did not include the Ca II H line since it was contaminated by a strong Balmer Hϵ feature. The mean McDonald S-index (SMcD, and not to be confused with the Mt. Wilson S-index) for β Gem is 0.118 ± 0.005 (see Sect. 2.3 in Paulson et al. 2002, for a detailed description of how the McDonald S-index for the Ca II K line core emission is obtained). This low value of the S-index is comparable to the inactive dwarf star τ Ceti (SMcD = 0.0166 ± 0.008). However, because of calibration issues it is probably not appropriate to compare the McDonald S-index between giants and dwarfs. On the other hand, support for the inactivity of β Gem comes from the X-ray flux for this star which is about a factor of 50 less than that of the solar value (Rutten et al. 1991).

For the purpose of confirming the nature of the RV variations we are not so much interested in the mean activity level of the star, but rather the *variability* of this level. The McDonald S-index which is calculated in a consistent way from the same dataset is appropriate for such an investigation. Figure 4 shows the the McDonald S-index measurements phased to orbital period. There are no obvious sinusoidal variations. The upper left panel of Fig. 5 shows the S-index measurements versus the RV measurement. The two quantities are uncorrelated having a correlation coefficient, r = 0.07 and a probability, $p_{\rm uncor}$ = 0.78 that they are uncorrelated.

K giant stars are known to exhibit variations in the Ca II core emission peaks, the ratio often denoted by V/R. For example, Arcturus shows variations in V/R from 0.80 to 1.05 (Gray 1980). The nature of these variations are not known. One possibility is variable mass loss (Chiu et al. 1977). Regardless of the cause, any variations in V/R that are correlated with the RV variations would cast doubt on the planet hypothesis. We measured the V/R ratio for the Ca II K line and these are plotted versus the RV measurement in the upper right panel of Fig. 5. Again there is no obvious correlation between the two quantities (r = 0.27, $p_{\rm uncor}$ = 0.27).

Finally, the total equivalent widths of the two K core emission peaks with respect to the flux level of the core of the line on

either side of the peaks were also measured. The variations of these with RV are shown in the lower left panel of Fig. 5. This quantity is also not correlated with the RV variations ($r = -0.03$, $p_{\rm uncor} = 0.9$). Our analysis of the Ca II data fails to support the hypothesis that the RV variations are due to magnetic (chromospheric) activity.

5.2. Spectral line bisector variations

The analysis of the shapes of spectral lines via line bisectors has proved to be an effective technique for confirming the planet hypothesis for RV variations. A lack of spectral line bisectors provided the final confirmation of the planet hypothesis to 51 Peg (Hatzes et al. 1998). Constant spectral line bisectors have established that sub-stellar companions were responsible for the RV variations in the K giants HD 47536 (Setiawan et al. 2003), HD 11977 (Setiawan et al. 2005), and HD 13189 (Hatzes et al. 2005).

To investigate whether β Gem exhibits line shape variations, observations were taken with the high resolution mode of the 2dcoudé spectrograph ($R = 210\,000$) on 10 different nights. The phase sampling of the data was good between phase 0 and 0.6, but with a large phase gap between 0.6–1.0. In spite of the large phase gap the phase coverage was sufficient to show any possible sinusoidal variations. Four to five exposures each with signal-to-noise levels of greater than 300 were taken. Spectral line bisectors were computed for 11 strong, unblended spectral features. For our bisector measurements we chose the spectral lines Fe I λ5379.6, Fe I λ5543.2, Fe I λ5637.4, Fe I λ5731.8, Fe I λ5934.7, Fe I λ6141.7, Fe I λ6151.6, Fe I λ6252.6, Fe I λ6254.2, Ca I λ6499.6, and Fe I λ6750.1. Two bisector quantities were measured: the velocity span which is the velocity difference between two endpoints of the bisector and the curvature which is the difference of the velocity span of the upper half of the bisector minus the lower half. We examined both quantities because it is possible for a star to show variations in one quantity but not the other. For our span measurements we chose flux levels of 0.40 and 0.85 of the continuum and 0.6 for the curvature measurement. These avoided the cores and wings of the spectral lines where the error of the bisector measurements are large. The average velocity span and curvature were computed for each spectral line and for each observation. After subtracting the mean value of the bisector span (curvature) for each line all bisectors quantities were averaged together to produce the mean for a given night. Thus approximately 50–60 individual bisector measurements (4–5 individual observations and 11 spectral lines) go into the computation of each mean value at a given orbital phase.

Figure 6 shows the resulting bisector velocity span and curvature measurements phased to the period found in the RV data. The error bars represent the standard error of the mean (standard deviation of measurements used for each average, divided by the square root of the number of measurements). There are no convincing sinusoidal RV variations in either the velocity span or curvature. A least squares sine fit to the data yields an amplitude of 2.5 ± 2.8 m s^{-1} for span variations and 0.40 ± 2.8 m s^{-1} for any curvature variations in the spectral line shapes. The lower right panel of Fig. 5 shows the bisector velocity span and curvature values versus the RV measurements. The correlation coefficient is 0.10 with a probability of 0.79 for the data not being correlated. Our analysis of the spectral line shapes also does not support rotational modulation by surface features or pulsations as a cause for the radial velocity variations.

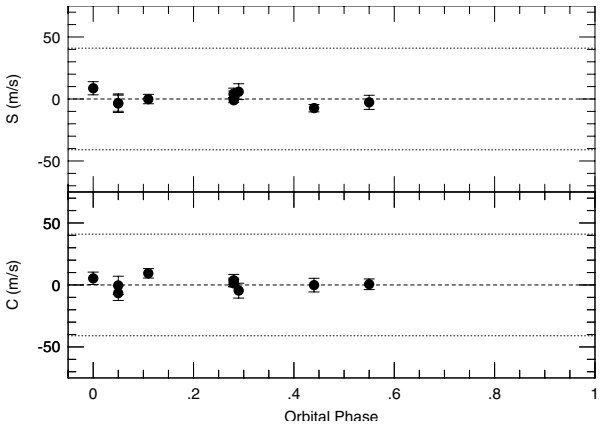

Fig. 6. The mean velocity span (*top*) and curvature (*bottom*) of the spectral line bisectors of β Gem as a function of orbital phase (590-day RV period). Dotted lines mark the maximum extent of the RV variations and the dashed line is the zero level.

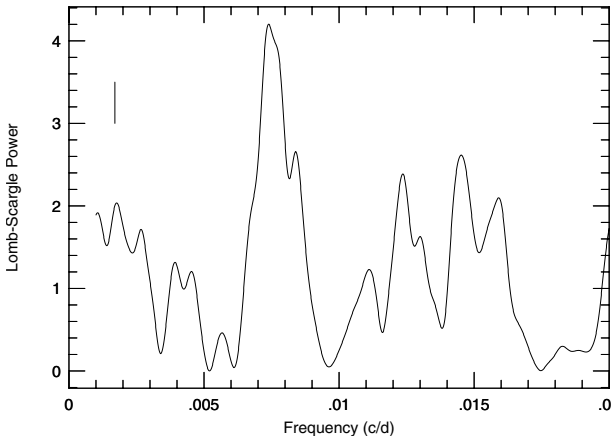

Fig. 7. The Lomb-Scargle periodogram of the Hipparcos photometry. The vertical line marks the orbital frequency.

5.3. Hipparcos photometry

The Hipparcos satellite made precise photometric measurements for β Gem that were contemporaneous with the RV measurements of our data set. Figure 7 shows the Lomb-Scargle periodogram of the Hipparcos photometry excluding one measurement with large error (four times the average error). The top panel of Fig. 8 shows this photometry phased to the 590-d orbital period. Although there is considerable scatter in the data there are no obvious sinusoidal variations. A sine fit to the photometry using the orbital period yields an amplitude of 3.03 ± 3.12 mmag for photometric variations with the RV period.

A least squares sine-fit was made to the Hipparcos photometry again excluding the one point with large error. This yielded a best fit period of 135 days, consistent with the highest peak of the periodogram. The lower panel of Fig. 8 shows the photometry phased to the 135-day period. If this period is indeed present then it most likely represents the rotation period of the star. More importantly, the Hipparcos photometry does not support rotational modulation as the cause of the RV variations.

We analyzed the residual RV variations after subtracting the Keplerian motion to see if we could detect any evidence of the 135-day photometric period in the RV measurements. Figure 9 shows the Lomb-Scargle periodogram of the residual RV variations excluding the lower precision DAO measurements. The highest peak is at a frequency corresponding to a period of

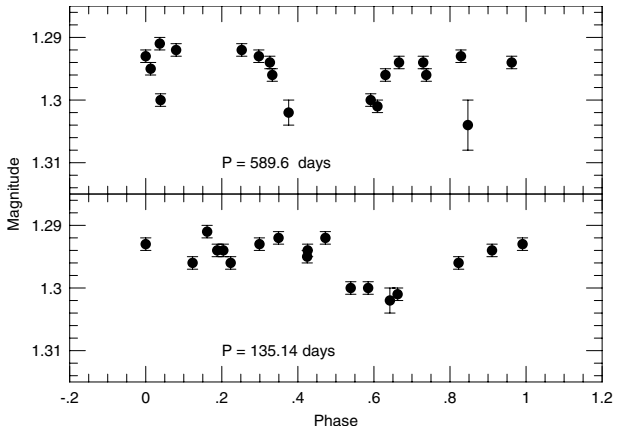

Fig. 8. The Hipparcos photometry for β Gem phased to the 590-d orbital period (*top*) and the best-fit 135-d period (*bottom*). The measurement with the large error was excluded in the lower panel.

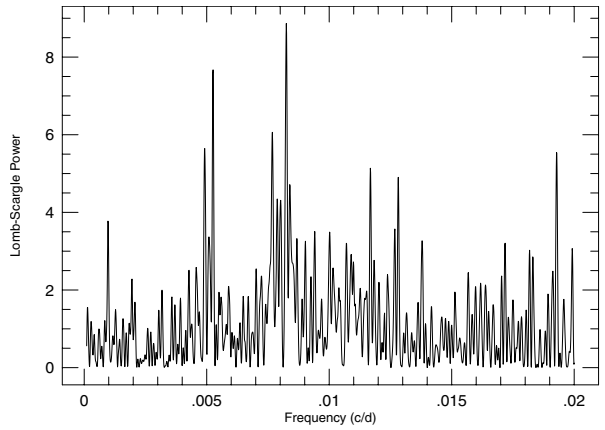

Fig. 9. The Lomb-Scargle Periodogram of the residual RV measurements after subtracting the contribution of the orbital motion due to the companion.

121 days. (The second highest peak is for a period of 190 days.) Although this is near the period of the best-fit sine wave to the photometric data we do not consider it as significant. The false alarm probability is 0.017 determined after 10 000 shuffles of the bootstrap randomization technique. (We consider a FAP < 0.001 to be a significant periodic signal.) However, both the Hipparcos photometry and the residual RV measurements show some evidence that the rotation period of β Gem may be ∼130 days.

6. Discussion

Our analysis of the radial velocity measurements for β Gem show that the long period variations found by HC93 and confirmed by Larson et al. (1993a) are long-lived and coherent. These RV variations have not changed in period, amplitude, or phase over the past 25 years. A careful examination of the Ca II K emission, spectral line shapes, and Hipparcos photometry reveals no convincing variation with the 590-day RV period. If the RV variations were due to stellar surface structure or stellar oscillations then it is difficult to reconcile the RV variations with a lack of spectral or photometric variability. Of course, we cannot entirely exclude that an exotic form of stellar oscillations could cause the RV variations. For example, toroidal modes have all of their atmospheric motion in the horizontal direction. These would produce no photometric or Ca II emission variations. However, these modes can produce line profile variations if the star is viewed from an intermediate inclination (Osaki 1986). Our bisector measurements exclude this possibility. The most likely and logical explanation for the RV variations is that they are indeed due to a planetary companion with minimum mass of 2.3 $M_\odot$ at an orbital distance of 1.6 AU. These data confirm the planet hypothesis for the long period RV variations first proposed by HC93.

If the 135-d period found in the Hipparcos photometry indeed represents the rotational period, then this can be used to estimate the stellar inclination. HC93 measured a projected rotational velocity for β Gem of 1.6 ± 0.9 km s^{-1}. A radius of 8.8 $R_\odot$ yields an equatorial rotational velocity of 3.3 km s^{-1}. This yields $\sin i = 0.48 \pm 0.3$. Assuming an alignment of rotational and orbital axes results in a true companion mass of 2.9–12.8 $M_{\rm Jupiter}$.

We can check if the possible photometric variations that are detected could result from rotation in spite of the low activity level of this star by comparing it with models. Given the period and velocity amplitude of the RV variations radial pulsations would produce a change in stellar radius of about 10%. This can be excluded by the lack of large photometric variations. Non-radial pulsations are ruled out by lack of bisector variations, and significant numbers of starspots would be surprising on such an inactive star (e.g., $F_{\rm X}/F_{\rm X}(\odot) \approx 0.02$; Rutten et al. 1991). The average solar spot coverage is $f_{\rm S} \sim 0.001$ ($\langle R_{\rm M} \rangle = 50$, $f_{\rm S} \approx 2.2 \times 10^{-5} R_{\rm M}$; Cox 2000). If $f_{\rm S}$ scales with $F_{\rm X}$, then for β Gem $f_{\rm S} \sim 2 \times 10^{-5}$, far too small to yield the photometric variability seen by Hipparcos ($\sigma_{\rm V} \approx 0.0033$).

A more likely possibility is microvariability due to the stellar granulation – specifically, due to the finite number of (variable) convective granules on the stellar surface. Ludwig (2006) estimates that the fractional flux rms σ_F/F due to granulation is given by (combining their Eqs. (56) and (59)):

$$\sigma_F/F = 0.4 N^{-0.5} (\delta I_{\rm rms}/I) f(a)$$

where N is the number of granules on the stellar surface, $\delta I_{\rm rms}/I$ is the fractional rms intensity variation due to a granule at $\mu = 1$, and $f(a)$ is a slowly varying function of the linear limb-darkening coefficient a. Freytag et al. (2002) use 3-D hydrodynamic models to show that the size of a typical granule scales with the pressure scale height as

$$x_{\rm gran}/R_* \approx 0.0025 (T_*/T\odot)(R_*/R_\odot)(M_*/M_\odot)^{-1}.$$

Thus, for β Gem $x_{\rm gran}/R_* \approx 0.015$, implying $N \sim 8900$ on the visible stellar surface. Then, if we adopt the solar value of $\delta I_{\rm rms}/I = 0.18$, and take $\epsilon = 0.8$, $f(a) \approx 1.3$, and $\sigma_F/F \sim 0.001$. While this a factor of ≈3 smaller than $\sigma_{\rm V}$, we feel the two are sufficiently close (given the many approximations involved) to suggest it is quite probable that the photometric variation is due to granulation-induced inhomogeneities combined with rotation.

β Gem with an estimated mass of 1.7 $M_\odot$ is the sixth star of intermediate mass known to host an extrasolar planet. Table 6 lists those stars in the mass range 1.8–5 $M_\odot$ known to host giant planets (ι Dra has an estimated mass of 1.05 $M_\odot$).

Although the number of intermediate mass stars hosting giant planets is small, these already show some interesting characteristics. First, all would qualify as "super planets" having masses much greater than a few Jupiter masses. Possibly, more massive stars have more massive protoplanetary disks which could result in more massive planets. Second, the semi-major axes for most are around 2 AU. This might raise concerns that we are seeing some other phenomena such as rotation and not evidence for planetary companions; however, we believe this is not the case for two reasons: 1) for these stars the RV variations

Table 6. Sub-stellar companions to intermediate mass stars.

Star	$M_{\rm star}$	$R_{\rm star}$	$M_{\rm planet}\times \sin i$	a	P	e	[Fe/H]
HD 11977[1]	1.9	10.2	6.5	1.9	1420	0.40	−0.14
HD 47536[2]	2.0	21.3	5.0	2.0	712	0.20	−0.61
HD 13189[3]	3.5	–	14	1.8	471	0.27	−0.59
HD 104985[4]	1.6	11	6.3	0.78	198	0.03	−0.35
γ Cep[5]	1.6	4.7	1.7	2.3	920	0.12	+0.18
β Gem	1.7	8.4	2.3	2.4	590	0.02	+0.19

[1] Setiawan et al. (2005); [2] Setiawan et al. (2003); [3] Hatzes et al. (2005); [4] Sato et al. (2003); [5] Hatzes et al. (2003).

were not accompanied by other forms of variations which excluded rotational modulation or pulsations as a cause. 2) The derived orbital eccentricities span a wide range (e = 0.01−0.40). If the RV variations were due to stellar rotation or pulsations, then we would not expect similar shapes in the RV curves and not the wide variety that is provided by Keplerian motion. Furthermore, not all K giant stars show long period RV variations. In a sample of 62 K giants Döllinger et al. (2006) found evidence for long period RV variations in at most 15% of stars.

Most of the stars in Table 6 have low metallicities. Rice & Armitage (2005) have argued that stars with lower metallicities take longer to form planets. These would have had little time to migrate before the disks were dispersed leaving the giant planets near the snow-line of ≈2–4 AU. However, β Gem and γ Cep have metallicities considerably higher than the solar value. Alternatively, radiation pressure from the more massive and thus hotter star may have dispersed the disks before the giant planet had time to migrate.

Another interesting trend in Table 6 is that most low metallicity stars have relatively eccentric orbits (the exception is HD 104985). Rice et al. (2003) argued that *if* the gravitational instability mechanism were to form planets, then the expected metallicity distribution of these would not be metal rich. It is interesting that this is consistent with Table 6. However, it is dangerous to draw conclusions based on such a small sample and any trends may just be coincidental. The sample of exoplanets around intermediate stars must be increased by at least an order of magnitude before we can discern the true distribution of semi-major axes and companion masses. Further discoveries of giant planets around intermediate stars may indeed hold important clues for planet formation.

Acknowledgements. We thank Carlos Allende-Prieto and Ken Rice for useful discussions. WDC and ME acknowledge the support of NASA grants NNG04G141G and NNG05G107G. SHS was supported by NASA Origins of Solar Systems grant NNG04GL54G. GAHW is supported by the Natural Sciences and Engineering Research Council of Canada. DBP is currently a NASA Postdoctoral fellow. The NASA Postdoctoral Program is administered by the Oak Ridge Associated Universities. This research has made use of the SIMBAD data base operated at CDS, Strasbourg, France.

References

Allende Prieto, C., & Lambert, D. L. 1999, A&A, 352, 555
Campbell, B., & Walker, G. A. H. 1979, PASP, 91, 540
Chiu. H. Y., Adams, P. J., Linsky, J. L., et al. 1977, ApJ, 211, 453
Cox, A. 2000, Allen's Astrophysical Quantities, Fourth Addition (New York: AIP Press, Springer-Verlag)
Döllinger, M., Pasquini, L., Hatzes, A., et al. 2006, in Tenth Anniversary of 51 Peg-b: Status of and Prospects for Hot Jupiter Studies. Proceedings of Haute Provence Observatory Colloquium (22–25 August 2005), ed. L. Arnold, F. Bouchy, & C. Moutou, Frontier Group, Paris, p. 138
Endl, M., Kürster, M., & Els, S. 2000, A&A, 362, 585
Freytag, B., Steffen, M., & Dorch, B. 2002, AN 323, 213
Frink, S., Mitchell, D. S., Quirrenbach, A., et al. 2002, ApJ, 576, 478
Gray, D. F. 1980, ApJ, 240, 125
Gray, R. O., Corbally, C. J., Garrison, R. F., McFadden, M. T., & Robinson, P. E. 2003. AJ, 126, 2048
Hatzes, A. P., & Cochran, W. D. 1993, ApJ, 413, 339 (HC93)
Hatzes, A. P., & Cochran, W. D. 1994a, ApJ, 422, 366
Hatzes, A. P., & Cochran, W. D. 1994b, ApJ, 432, 763
Hatzes, A. P., Cochran, W. D., & Bakker, E. J. 1998, Nature, 391, 154
Hatzes, A. P., Guenther, E. W., Endl, M., et al. 2005, A&A, 437, 743
Kim, K. M., Mkrtichian, D. E., Han, I., & Hatzes, A. P. 2006, A&A, 454, 839
Kürster, M., Schmitt, J. H. M. M., Cutispoto, G., & Dennerl, K. 1997, A&A, 320, 831
Larson, A. M., Irwin, A. W., Yang, S. L. S., et al. 1993a, PASP, 105, 332
Larson, A. M., Irwin, A. W., Yang, S. L. S., et al. 1993b, PASP, 105, 825
Lomb, N. R. 1976, Ap&SS, 39, 477
Ludwig, H.-G. 2006, A&A 445, 661
McWilliam, A. 1990, ApJS, 74, 1075
Murdoch, K. A., Hearnshaw, J. B., & Clark, M. 1993, ApJ, 413, 349
Nordgren, T. E., Sudol, J. J., & Mozurkewich, D. 2001, AJ, 122, 2707
Osaki, Y. 1986, in Seismology of the Sun and Distant Stars, ed. D.O. Gough (D. Reidel Publ. Co., Dordrecht), 453
Paulson, D. B., Saar, S. H., Cochran, W. D., & Hatzes, A. P. 2002, AJ, 124, 572
Rice, W. K. M., & Armitage, P. J. 2005, ApJ, 630, 1107
Rice, W. K. M., Armitage, P. J., Bonnel, I. A., et al. 2003, MNRAS, 346, L36
Rutten, R. G. M., Schrijver, C. J., Lemmens, A. F. P., & Zwaan, C. 1991, A&A, 252, 203
Sato, B., Ando, H., Kambe, E., et al. 2003, ApJ, 597, L157
Scargle, J. D. 1982, ApJ, 263, 835
Setiawan, J., Hatzes, A. P., von der Lühe, O., et al. 2003, A&A, 398, L19
Setiawan, J., Rodmann, J., da Silva, L., et al. 2005, A&A, 437, L31
Tull, R. G., MacQueen, P. J., Sneden, C., & Lambert, D. L. 1995, PASP, 107, 251

Online Material

Table 2. Radial Velocity Measurements for β Gem from the McDonald Phase III program (MOPS).

JD	*RV* (m/s)	σ (m/s)
2 451 558.8477	−25.93	5.0
2 451 624.7461	−19.67	4.3
2 451 655.5820	13.34	9.6
2 451 656.5898	−36.34	3.9
2 451 658.5938	−26.64	7.3
2 451 686.6055	−21.78	3.3
2 452 577.0117	17.86	3.4
2 452 597.9805	15.74	5.3
2 452 619.9531	1.93	5.5
2 452 658.8828	−23.03	4.9
2 452 661.7227	−34.38	4.5
2 452 688.8594	−35.57	4.3
2 452 742.5938	−36.13	4.0
2 452 743.5938	−50.45	3.2
2 452 931.0078	18.27	6.4
2 453 017.8711	45.97	5.2
2 453 320.0078	−38.81	5.6
2 453 436.6523	−28.23	3.7
2 453 636.9766	47.20	6.0
2 453 689.9219	39.20	5.4
2 453 746.9062	21.60	5.1
2 453 747.8125	11.56	4.0

Table 3. Radial Velocity Measurements for β Gem taken with the high resolution mode of the 2dcoudé spectrometer.

JD	*RV* (m/s)	σ (m/s)
2 450 836.7266	3.72	6.4
2 450 939.6445	−8.38	9.0
2 451 522.9219	−26.92	7.2
2 451 523.9141	−29.07	4.8
2 451 525.9219	−30.54	5.0
2 451 620.7695	−64.17	4.9
2 451 683.6562	−32.67	5.2
2 451 980.7500	24.25	4.3
2 451 981.6406	15.37	5.4
2 452 189.9844	−32.17	8.4
2 452 565.0000	−6.17	5.6

Table 4. Radial Velocity Measurements for β Gem from TOPS.

JD	*RV* (m/s)	σ (m/s)
2 452 656.6562	−22.87	3.5
2 452 683.2109	−21.72	2.5
2 452 744.2891	−36.09	3.1
2 452 746.2969	−37.64	2.8
2 452 751.2891	−35.31	2.1
2 452 752.2930	−35.72	2.1
2 452 753.2969	−22.83	3.5
2 452 782.8359	−36.32	2.6
2 452 783.3359	−31.51	4.4
2 452 877.6172	−14.63	2.9
2 452 929.6055	−9.30	5.0
2 452 952.5391	34.42	3.2
2 453 076.2656	34.23	2.4
2 453 080.3047	37.66	3.3
2 453 420.3789	−42.72	2.9
2 453 429.3594	−18.47	6.8
2 453 431.3477	−30.56	4.5
2 453 658.6523	22.47	5.5
2 453 661.6055	28.74	8.0
2 453 662.6680	22.77	5.0
2 453 750.4609	30.94	2.6
2 453 758.3281	25.43	3.0